Article

A Peptide Dendrimer Enzyme Model with a Single Catalytic Site at the Core

Sacha Javor, Estelle Delort, Tamis Darbre, and Jean-Louis Reymond

J. Am. Chem. Soc., **2007**, 129 (43), 13238-13246• DOI: 10.1021/ja074115f • Publication Date (Web): 09 October 2007

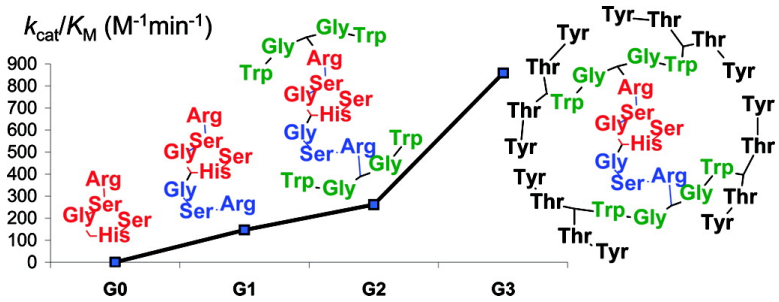

More About This Article

Additional resources and features associated with this article are available within the HTML version:

- Supporting Information
- Links to the 4 articles that cite this article, as of the time of this article download
- Access to high resolution figures
- Links to articles and content related to this article
- Copyright permission to reproduce figures and/or text from this article

View the Full Text HTML

J|A|C|S
ARTICLES
Published on Web 10/09/2007

A Peptide Dendrimer Enzyme Model with a Single Catalytic Site at the Core

Sacha Javor, Estelle Delort, Tamis Darbre,* and Jean-Louis Reymond*

Contribution from the Department of Chemistry and Biochemistry, University of Berne, Freiestrasse 3, 3012 Berne, Switzerland

Received June 23, 2007; E-mail: jean-louis.reymond@ioc.unibe.ch

Abstract: Catalytic esterase peptide dendrimers with a core active site were discovered by functional screening of a 65 536-member combinatorial library of third-generation peptide dendrimers using fluorogenic 1-acyloxypyrene-3,6,8-trisulfonates as substrates. In the best catalyst, **RMG3**, $((AcTyrThr)_8(DapTrpGly)_4(DapArgSerGly)_2DapHisSerNH_2)$, ester hydrolysis is catalyzed by a single catalytic histidine residue at the dendrimer core. A pair of arginine residues in the first-generation branch assists substrate binding. The catalytic proficiency of dendrimer **RMG3** ($k_{cat}/K_M = 860\ M^{-1}\ min^{-1}$ at pH 6.9) per catalytic site is comparable to that of the multivalent esterase dendrimer **A3** $((AcHisSer)_8(DapHisSer)_4(DapHisSer)_2DapHisSerNH_2)$ which has fifteen histidines and five catalytic sites (Delort, E. et al. *J. Am. Chem. Soc.* **2004**, *126*, 15642−15643). Remarkably, catalysis in the single site dendrimer **RMG3** is enhanced by the outer dendritic branches consisting of aromatic amino acids. These interactions take place in a relatively compact conformation similar to a molten globule protein as demonstrated by diffusion NMR. In another dendrimer, **HG3** $((AcIlePro)_8(DapIleThr)_4(DapHisAla)_2DapHisLeuNH_2)$ by contrast, catalysis by a core of three histidine residues is unaffected by the outer dendritic layers. Dendrimer **HG3** or its core **HG1** exhibit comparable activity to the first-generation dendrimer **A1** $((AcHisSer)_2DapHisSerNH_2)$. The compactness of dendrimer **HG3** in solution is close to that a denatured peptide. These experiments document the first esterase peptide dendrimer enzyme models with a single catalytic site and suggest a possible relationship between packing and catalysis in these systems.

Introduction

The catalytic function of enzymes arises through the relative positioning of functional groups in space to create a catalytic site. Designing enzymes *de novo* is one of the most challenging tasks in macromolecular chemistry. Most approaches to create functional analogues of enzymes are based on modifying the enzymes themselves or other proteins,[1] for example by selection for transition state analogue binding,[2] by directed evolution,[3] or by computational protein design.[4] Artificial enzymes may also be formed by design or functional selection from folded linear peptides[5] or noncatalytic proteins.[6] Additional strategies[1] include cofactor engineering,[7] the installation of cofactors or catalytic metal complexes into noncatalytic proteins,[8] and the search for promiscuous enzyme activities by active site or substrate modifications.[9]

The dendrimer approach to artificial enzymes follows a different strategy, belonging to the general theme of synthetic enzyme models,[10] and proposes to organize building blocks into a globular macromolecule by means of topology rather than by folding.[11] Most experiments toward catalytic dendrimers addressed the multivalent display of catalytic groups at the end of the dendritic branches,[12] which was found in several cases to enhance catalysis by cooperative multivalency effects despite steric crowding, following earlier reports in polymers with multiple catalytic and binding groups investigated as hydrolase mimics.[13] In the context of catalysis in aqueous medium, we recently reported strong enhancement of the catalytic potency of histidine and N-terminal proline residues by multivalent

(1) Toscano, M. D.; Woycechowsky, K. J.; Hilvert, D. *Angew. Chem., Int. Ed.* **2007**, *46*, 3212−3236.
(2) (a) Lerner, R. A.; Benkovic, S. J.; Schultz, P. G. *Science* **1991**, *252*, 659−667. (b) Schultz, P. G.; Lerner, R. A. *Acc. Chem. Res.* **1993**, *26*, 391−395. (c) Schultz, P. G.; Lerner, R. A. *Science* **1995**, *269*, 1835−1842. (d) MacBeath, G.; Hilvert, D. *Chem. Biol.* **1996**, *3*, 433−445. (e) Thomas, N. R. *Nat. Prod. Rep.* **1996**, *13*, 479−511. (f) Stevenson, J. D.; Thomas, N. R. *Nat. Prod. Rep.* **2000**, *17*, 535−537. (g) Keinan, E., Ed. *Catalytic Antibodies*; Wiley-VCH: Weinheim, 2005.
(3) (a) Reetz, M. T. *Angew. Chem., Int. Ed.* **2001**, *40*, 284−310. (b) Bloom, J. D.; Meyer, M. M.; Meinhold, P.; Otey, C. R.; MacMillan, D.; Arnold, F. H. *Curr. Opin. Struct. Biol.* **2005**, *15*, 447−452.
(4) (a) Bolon, D. N.; Voigt, C. A.; Mayo, S. L. *Curr. Opin. Chem. Biol.* **2002**, *6*, 125−129. (b) Kuhlman, B.; Baker, D. *Curr. Opin. Struct. Biol.* **2004**, *14*, 89−95. (c) Dwyer, M. A.; Hellinga, H. W. *Curr. Opin. Struct. Biol.* **2004**, *14*, 495−504. (d) Moffet, D. A.; Hecht, M. H. *Chem. Rev.* **2001**, *101*, 3191−3203.
(5) Berkessel, A. *Curr. Opin. Chem. Biol.* **2003**, *7*, 409−419.
(6) (a) Qi, D.; Tann, C.-M.; Haring, D.; Distefano, M. D. *Chem. Rev.* **2001**, *101*, 3081−3112. (b) Andersson, L. K.; Caspersson, M.; Baltzer, L. *Chem. Eur. J.* **2002**, *8*, 3687−3689.
(7) (a) van de Velde, F.; Arends, I. W.; Sheldon, R. A. *J. Inorg. Biochem.* **2000**, *80*, 81−89. (b) Wahler, D.; Reymond, J.-L. *Can. J. Chem.* **2002**, *80*, 665−670.
(8) Thomas, C. M.; Ward, T. R. *Chem. Soc. Rev.* **2005**, *34*, 337−346.
(9) Hult, K.; Berglund, P. *Curr. Opin. Biotechnol.* **2003**, *14*, 395−400.
(10) (a) Kirby, A. J. *Angew. Chem., Int. Ed.* **1996**, *35*, 706−724. (b) Woggon, W.-D. *Acc. Chem. Res.* **2005**, *38*, 127−136. (c) Motherwell, W. B.; Bingham, M. J.; Six, Y. *Tetrahedron* **2001**, *57*, 4663−4686. (d) Breslow, R.; Zhang, X.; Huang, Y. *J. Am. Chem. Soc.* **1997**, *119*, 4535−4536. (e) Breslow, R.; Huang, Y.; Zhang, X.; Yang, J. *Proc. Natl. Acad. Sci. U.S.A.*, **1997**, *94*, 11156−11158.

10.1021/ja074115f CCC: $37.00

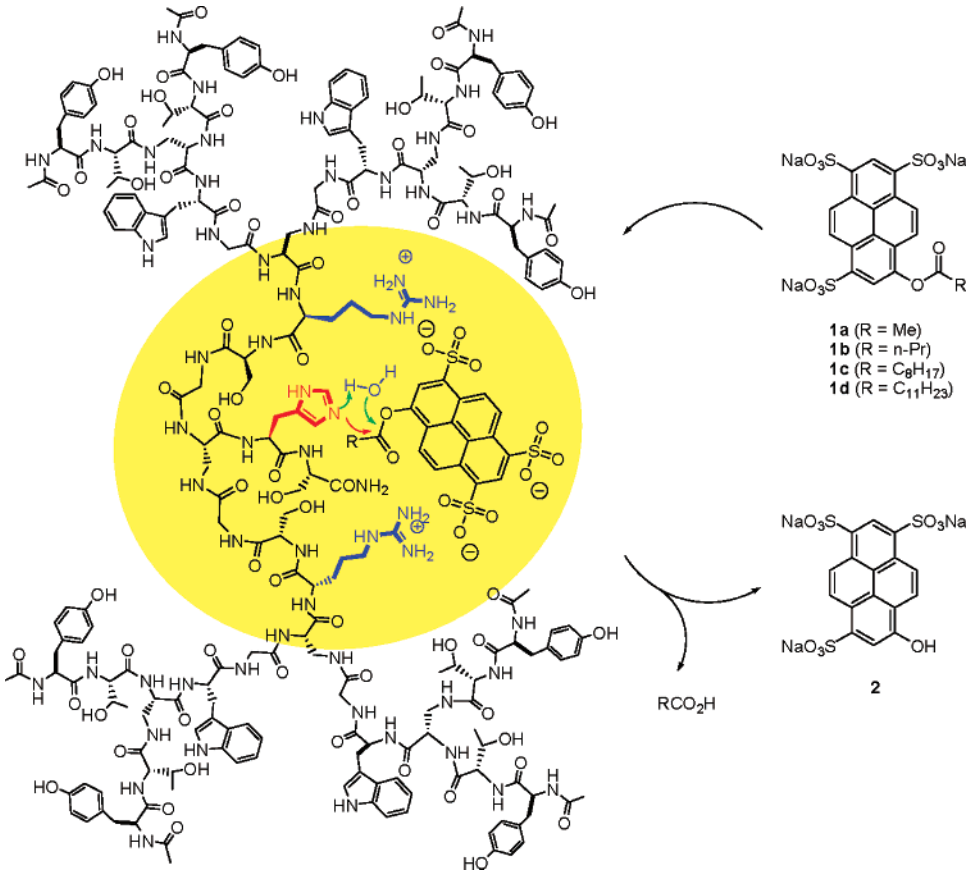

Figure 1. Esterase peptide dendrimer **RMG3** catalyzed hydrolysis of pyrene trisulfonate esters (green arrows indicate a possible general base mechanism; red arrow indicates an alternative nucleophilic catalysis). The yellow circle highlights the reactive core with substrate.

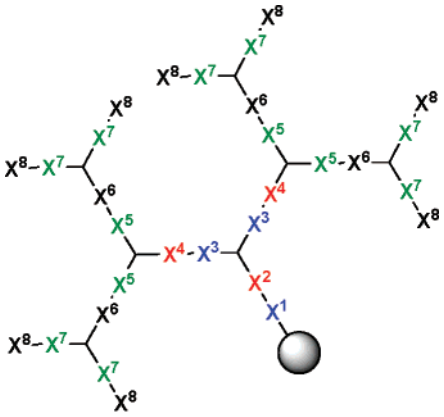

X^8, X^6	X^7, X^5	X^4, X^2	X^3, X^1
Tyr	Thr	His	Ser
Ile	Pro	Arg	Asp
Trp	Phe	Cys	Leu
Glu	Gly	Val	Ala

Figure 2. Combinatorial library of 65 536 peptide dendrimers. The branching points consist of (*S*)-2,3-diaminopropanoic acid (Dap). All N-terminal positions are acetylated. The solid support in the library is tentagel with an ϵ-aminohexanoylglycine spacer.

display within peptide dendrimers[14] for the catalysis of ester hydrolysis[15,16] and aldol reactions,[17] respectively.

Other studies of catalytic dendrimers have addressed the possible enhancement of the catalytic properties of a metal complex or functional group placed at the dendritic core by grafting dendritic branches around it, in the spirit of creating dendritic enzyme mimics with a single catalytic site.[12a−d] It is indeed the hallmark of natural enzymes that the bulk of the protein is able to enhance the efficiency of a few catalytic residues placed at the active site not by providing additional catalytic functionality but rather through indirect effects such as directed substrate binding, preorganization of catalytic residues, and polarization effects stabilizing the transition state.[18]

(11) (a) Newkome, G. R.; Moorefield, C. N.; Vögtle, F. *Dendritic Molecules: Concepts, Synthesis, Applications*; VCH: Weinheim, 2001. (b) Tomalia, D. A.; Dvornic, P. R. *Nature* **1994**, *372*, 617−618. (c) Smith, D. K.; Diederich, F. *Top. Curr. Chem.* **2000**, *210*, 183−227. (d) Helms, B.; Fréchet, J. M. J. *Adv. Synth. Catal.* **2006**, *348*, 1125−1148. (e) Smith, D. K.; Diederich, F. *Chem. Eur. J.* **1998**, *4*, 1353−1361. (f) Liang, C.; Fréchet, J. M. J. *Prog. Polym. Sci.* **2005**, *30*, 385−402. Grayson, S. M.; Fréchet, J. M. J. *Chem. Rev.* **2001**, *101*, 3819−3868. (g) Lee, C. C.; Mackay, J. A.; Fréchet, J. M. J.; Szoka, F. C. *Nat. Biotechnol.* **2005**, *23*, 1517−1526.

(12) Reviews on catalysis with dendrimers: (a) Oosterom, G. E.; Reek, J. N.; Kamer, P. C.; van Leeuwen, P. W. *Angew. Chem., Int. Ed.* **2001**, *40*, 1828−1849. (b) Twyman, L. J.; King, A. S.; Martin, I. K. *Chem. Soc. Rev.* **2002**, *31*, 69−82. (c) Kofoed, J.; Reymond, J.-L. *Curr. Opin. Chem. Biol.* **2005**, *9*, 656−664. (d) Astruc, D.; Heuze, K.; Gatard, S.; Mery, D.; Nlate, S.; Plault, L. *Adv. Synth. Catal.* **2005**, *347*, 329−338. (e) Helms, B.; Fréchet, J. M. J. *Adv. Synth. Catal.* **2006**, *348*, 1125−1148. Recent reports: (f) Wang, Z.-J.; Deng, G.-J.; Yong, L.; He, Y.-M.; Tang, W.-J.; Fan, Q.-H. *Org. Lett.* **2007**, *9*, 1243−1246. (g) Ouali, A.; Laurent, R.; Caminade, A. M.; Majoral, J.-P.; Taillefer, M. *J. Am. Chem. Soc.* **2006**, *128*, 15990−15991. (h) van de Coevering, R.; Alfers, A. P.; Meeldijk, J. D.; Martinez-Viviente, E.; Pregosin, P. S.; Klein, Gebbink, R. J. M.; van Koten, G. *J. Am. Chem. Soc.* **2006**, *128*, 12700−12713. (i) Abu-Reziq, R.; Alper, H.; Wang, D.; Post, M. L. *J. Am. Chem. Soc.* **2006**, *128*, 5279−5282.

(13) For early examples of catalytic polymers with imidazole groups: (a) Overberger, C. G.; Salamone, J. C. *Acc. Chem. Res.* **1969**, *2*, 217−224. (b) Overberger, C. G.; Mitra, S. *Pure Appl. Chem.* **1979**, 51, 1391−1404. For other examples and reviews: (c) Suh, J. *Acc. Chem. Res.* **2003**, *36*, 562−570. (d) Benaglia, M. Puglisi.; Cozzi, F. *Chem. Rev.* **2003**, *103*, 3401−3429. (e) Bosman, A. W.; Vestberg, R.; Heumann, A.; Fréchet, J. M. J.; Hawker, C. J. *J. Am. Chem. Soc.* **2003**, *123*, 5908−5917.

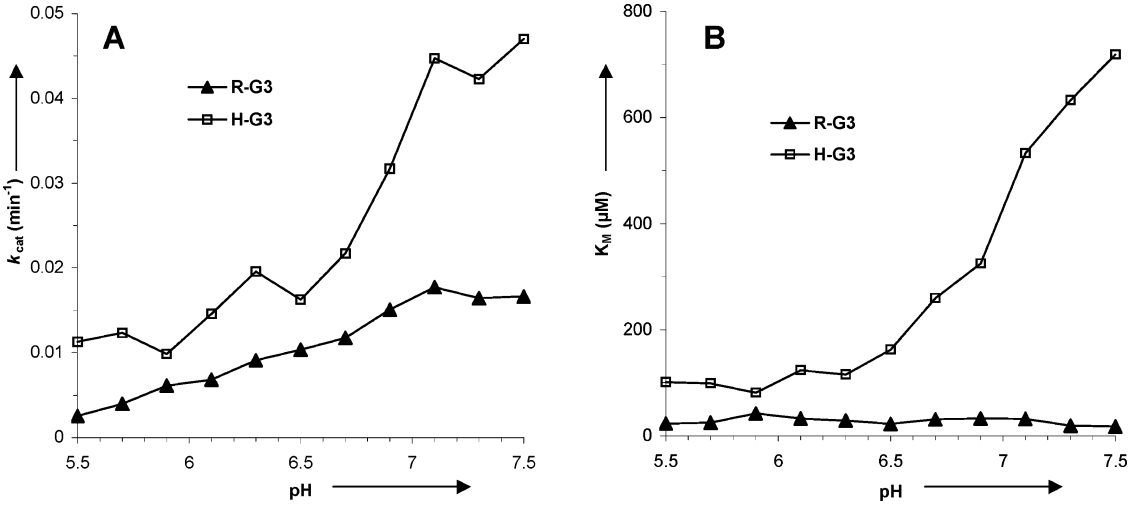

Figure 3. pH-profile of catalytic parameter for dendrimer **RG3** (●) and **HG3** (▲) catalyzed hydrolysis of butyrate **1b**. A: Catalytic rate constant k_{cat}. B: Michaelis constant K_M. Conditions: 5.0 μM dendrimer, 29−1000 μM **1b**, 10 mM Bis-Tris buffer, 34 °C.

Table 1. Peptide Dendrimer Sequences Identified by Amino Acid Analyses of Active Beads from Selection Assay on Substrate **1b**[a]

no.	intensity[b]	X^8	X^7	X^6	X^5	X^4	X^3	X^2	X^1
1	++	I	F	W	G	H	A	R	A
2	++	I	P	I	T	**H**	A	C	S
3	++	I	T	I	P	C	S	R	L
4	++	I	T	W	P	R	A	C	S
5	+	I	F	W	G	**H**	A	R	A
6	+	I	T	Y	G	R	S	C	L
7	++	Y	T	I	T	R	S	C	S
8	+	Y	T	I	F	R	L	C	L
9	++	Y	P	Y	G	**H**	S	**H**	L
10	++	Y	F	Y	G	R	D	R	L
11	++	I	T	Y	T	**H**	A	**H**	A
12	+	I	F	Y	G	**H**	L	**H**	L
13	++	I	T	Y	T	**H**	A	C	L
14	+	Y	G	Y	T	R	S	C	S
15	+	I	P	I	F	R	L	V	S
16 (**RG3**)	+++	Y	T	W	G	R	S	**H**	S

[a] Conditions: 45 mg batch of on-bead library swollen in 500 μL Bis-Tris pH 6.0 (20 mM) for 40 min, then mixed with 500 μL of substrate **1b** (80 μM in Bis-Tris pH 6.0) for 8 min, then spread on a silica plate, UV irradiation 365 nm. [b] + weak fluorescence, ++ strong fluorescence, +++ very strong fluorescence.

To date there are only very few examples where addition of dendritic branches to a catalytic core resulted in significant increases in rates or selectivity. These include catalysis of transamination by a dendritic pyridoxal cofactor,[19] the catalysis of singlet oxygen cycloaddition by a dendritic benzophenone,[20] and catalysis of transesterification by a dendritic 4-pyrrolidinopyridine.[21] Unimolecular dendritic reverse micelles have also been shown to catalyze the dehydrohalogenation of 2-iodo-2-methylheptane with high turnover.[22] In each case the rate enhancement effect was attributed to the effect of the nanoenvironment on substrate binding and/or transition state stabilization.

Herein we report the first catalytic peptide dendrimers with a single catalytic site at the core as an example of an ester hydrolysis reaction. These dendrimers were discovered by activity screening of combinatorial dendrimer libraries using our recently reported method for the synthesis and decoding of such libraries.[23] We have used this approach previously to discover multivalent esterase[23] and aldolase[17] dendrimers, as well as multivalent lectin binding glycodendrimers.[24] The library used here to discover single site catalytic dendrimers features catalytic amino acids at the core and noncatalytic residues in the outer shells to provide a favorable protein-like environment.

(14) (a) Crespo, L.; Sanclimens, G.; Pons, M.; Giralt, E.; Royo, M.; Albericio, F. *Chem. Rev.* **2005**, 1663−1681. (b) Sadler, K.; Tam, J. P. *Rev. Mol. Biotechnol.* **2002**, *90*, 195−229. (c) Darbre, T.; Reymond, J.-L. *Acc. Chem. Res.* **2006**, *39*, 925−934.
(15) (a) Esposito, A.; Delort, E.; Lagnoux, D.; Djojo, F.; Reymond, J.-L. *Angew. Chem., Int. Ed.* **2003**, *42*, 1381−1383. (b) Lagnoux, D.; Delort, E.; Douat-Casassus, C.; Esposito, A.; Reymond, J.-L. *Chem. Eur. J.* **2004**, *10*, 1215−1226. (c) Douat-Casassus, C.; Darbre, T.; Reymond, J.-L. *J. Am. Chem. Soc.* **2004**, *126*, 7817−7826. (d) Clouet, A.; Darbre, T.; Reymond, J.-L. *Adv. Synth. Catal.* **2004**, *346*, 1195−1204.
(16) (a) Delort, E.; Darbre, T.; Reymond, J.-L. *J. Am. Chem. Soc.* **2004**, *126*, 15642−15643. (b) Delort, E.; Nguyen-Trung, N.-Q.; Darbre, T.; Reymond, J.-L. *J. Org. Chem.* **2006**, *71*, 4468−4480.
(17) Kofoed, J.; Darbre, T.; Reymond, J.-L. *Org. Biomol. Chem.* **2006**, 3268−3281.
(18) (a) Warshel, A.; Florian, J. *Proc. Natl. Acad. Sci. U.S.A.* **1998**, *95*, 5950−5955. (b) Bruice, T. C. *Chem. Rev.* **2006**, *106*, 3119−3139. (c) Benkovic, S. J.; Hammes-Schiffer, S. *Science* **2003**, *301*, 1196−1202.
(19) Liu, L.; Breslow, R. *J. Am. Chem. Soc.* **2003**, *125*, 12110−12111.
(20) Hecht, S.; Fréchet, J. M. J. *J. Am. Chem. Soc.* **2001**, *123*, 6959−6960.
(21) Liang, C. O.; Helms, B.; Craig, J.; Frechet, J. M. J. *Chem. Commun.* **2003**, 2524−2525
(22) Piotti, M. E.; Rivera, F., Jr.; Bond, R.; Hawker, C. J.; Fréchet, J. M. J. *J. Am. Chem. Soc.* **1999**, *121*, 9471−9472.
(23) (a) Clouet, A.; Darbre, T.; Reymond, J.-L. *Angew. Chem., Int. Ed.* **2004**, *43*, 4612−4615. (b) Clouet, A.; Darbre, T.; Reymond, J.-L. *Biopolymers* **2006**, *84*, 114−123.
(24) (a) Kolomiets, E.; Johansson, E. M. V.; Renaudet, O.; Darbre, T.; Reymond, J.-L. *Org. Lett.* **2007**, *9*, 1465−1468. (b) Johansson, E. M. V.; Kolomiets, E.; Rosenau, F.; Jäger, K.-E.; Darbre, T.; Reymond, J.-L. *New J. Chem.* **2007**, *31*, 1291−1299.

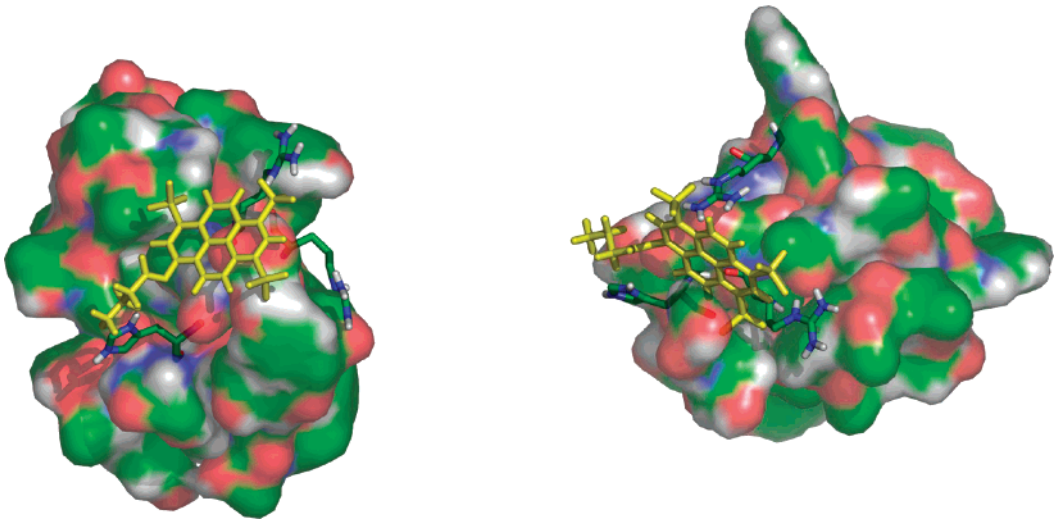

Figure 4. Space filling model of a minimized energy conformation of dendrimer **RG3** (left) and **RMG3** (right). The pyrene trisulfonate substrate **1b** was placed manually on the surface. The arginine and histidine residues are shown in stick model and the dendrimer in molecular surface representation colored by atom type (green: carbon; white: hydrogen; red: oxygen; blue: nitrogen). The image was generated from coordinates produced by GROMACS using PyMol.[29] Energy-minimized conformations were computed at pH 7 in water (SPC model) as explicit solvent by gradual cooling from 800 to 300 K over 180 ps. Similar relative arrangement of histidine and arginine side chains, compatible with the proposed mechanism, were observed in the energy-minimized conformations at 300 K generated from 20 different starting conformations sampled at 800 K.

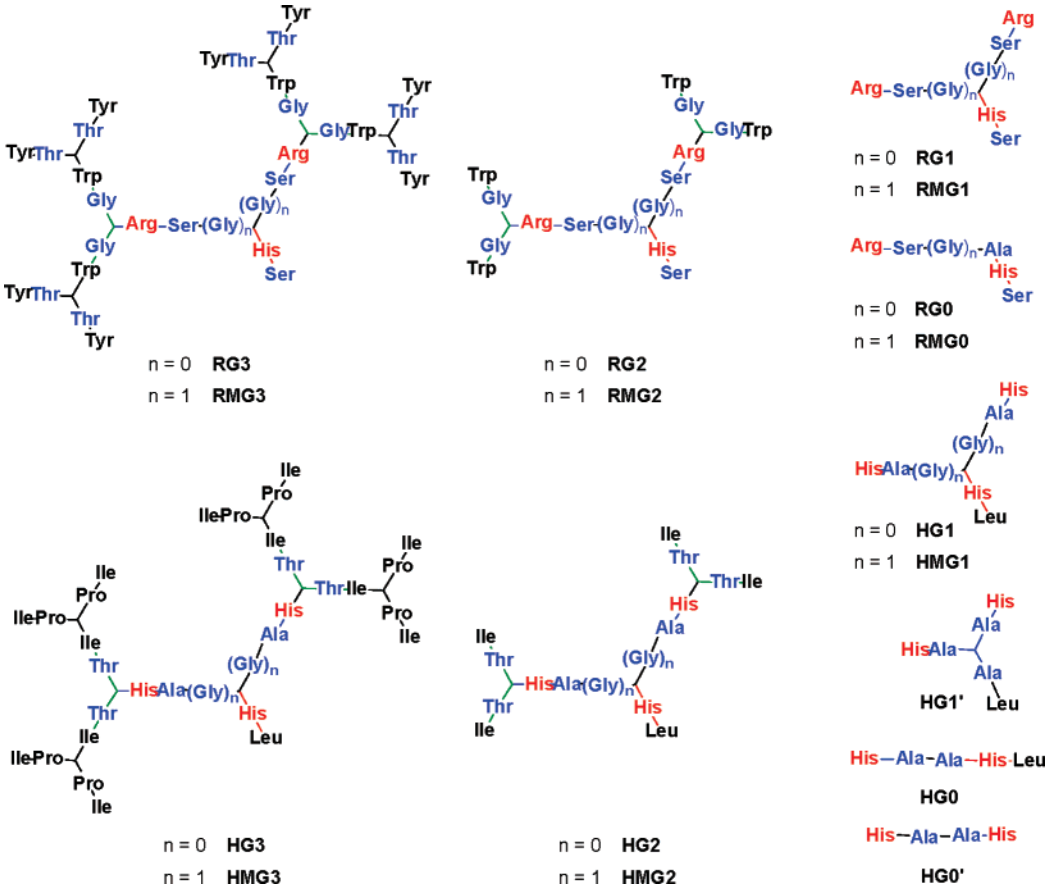

Figure 5. Esterase dendrimers and analogues. The branching points consist of (*S*)-2,3-diaminopropanoic acid (Dap). All sequences are acetylated at the N-termini and have their C-terminus as amide ($CONH_2$).

The dendrimers catalyze the hydrolysis of 1-acyloxypyrene-3,6,8-trisulfonates **1a/b** in aqueous buffer. In the best catalyst identified, **RMG3** catalysis by the dendritic core is enhanced by the outer layers of aromatic amino acids (Figure 1). The reactivity enhancement effect on the catalytic histidine residue in this single-site system is comparable to the effect observed per catalytic site in our previously reported multivalent esterase dendrimer system.[16a] Dendrimer **RMG3** adopts a globular conformation in solution with packing similar to a molten globule protein as demonstrated by diffusion NMR measurements. A second catalytic dendrimer, **HG3**, featuring a hydrophobic aliphatic outer layer shows no catalysis enhancement

Table 2. Peptide Dendrimer Sequences Identified by Amino Acid Analysis of Active Beads from Selection Assay on Substrate **1d**[a]

no.	intensity[b]	X^8	X^7	X^6	X^5	X^4	X^3	X^2	X^1
1	+++	Y	T	I	T	**H**	A	**H**	A
2	+++	W	F	I	T	**H**	A	**H**	L
3	++	Y	P	I	T	**H**	A	V	S
4	+	Y	T	I	T	**H**	A	V	S
5	+	I	P	I	T	**H**	A	**H**	S
6	+	Y	F	I	T	**H**	S	**H**	L
7	+	Y	F	I	T	**H**	S	V	S
8	++	I	T	Y	T	**H**	A	**H**	L
9 (**HG3**)	++	I	P	I	T	**H**	A	**H**	L
10	+	Y	F	I	T	**H**	S	R	S
11	+	Y	T	I	G	**H**	A	H	L
12	+++	I	P	W	T	**H**	A	**H**	S
13	++	I	T	W	T	**H**	A	**H**	L
14	+	Y	T	I	T	**H**	A	**H**	S
15	+	I	P	I	T	**H**	A	**H**	A

[a] Conditions: Same as in Table 1 using substrate **1d**. [b] + weak fluorescence, ++ strong fluorescence, +++ very strong fluorescence.

Table 3. Synthesis of Core Active Site Esterase Dendrimers and Analogues

no.	sequence	yield (%)	*m* (mg)	MS calcd	MS obsd[a]
R-G0	AcRSAHS	2.2	2.9	598.3	598.6
R-G1	$(AcRS)_2BHS$	27.5	8.5	898.5	897.4
R-G2	$(AcWG)_4(BRS)_2BHS$	5.4	3.3	2127.0	2126.8
R-G3	$(AcYT)_8(BWG)_4(BRS)_2BHS$	1.7	5.5	4752.1	4754.4
RMG0	AcRSGAHS	50.6	70.4	655.3	655.4
RM-G1	$(AcRSG)_2BHS$	51.9	40.4	1012.5	1012.8
RM-G2	$(AcWG)_4(BRSG)_2BHS$	5.2	7.7	2241.0	2241.5
RM-G3	$(AcYT)_8(BWG)_4(BRSG)_2BHS$	7.3	24.8	4866.1	4868.7
H-G0	AcHAAHL	61.4	78.8	589.3	589.4
H-G0′	AcHAAH	60.9	67.3	476.2	476.4
H-G1′	$(AcHA)_2BAL$	45.9	73.3	788.4	788.6
H-G1	$(AcHA)_2BHL$	58.7	40.4	854.4	854.6
H-G2	$(AcIT)_4(BHA)_2BHL$	7.7	10.2	1967.1	1967.4
H-G3	$(AcIP)_8(BIT)_4(BHA)_2BHL$	16.0	46.7	4160.4	4162.2
HM-G1	$(AcHAG)_2BHL$	53.2	40.1	968.5	968.6
HM-G2	$(AcIT)4(BHAG)_2BHL$	25.5	35.5	2081.1	2081.4
HM-G3	$(AcIP)_8(BIT)_4(BHAG)_2BHL$	9.5	28.6	4274.5	4277.4

[a] (ES+) $[M + H]^+$ peak. For the complete ion interpretation, see Supporting Information. *B* = branching unit (*S*)-2,3-diaminopropanoic acid (Dap). Amino acids indicated with one-letter code.

by the outer layers, and a less compact conformation closer to a denatured peptide.

Results and Discussion

To search for a core-active site peptide dendrimer enzyme model, we focused our attention on the hydrolysis of 1-acyloxypyrene-3,6,8-trisulfonates **1a**−**d**, which is a favorable model reaction for the study of aqueous esterolysis. These fluorogenic pyrene substrates render direct on-bead screening possible and facilitate kinetic studies. Furthermore, the reaction is catalyzed by 4-methylimidazole and therefore should require only a single histidine side chain for catalysis. Nevertheless, dendrimers with a single catalytic histidine at their core, such as $(Ac\text{-}Ala\text{-}Ser)_8$-$(Dap\text{-}Ala\text{-}Ser)_4(Dap\text{-}Ala\text{-}Ser)_2Dap\text{-}His\text{-}Ser\text{-}NH_2$, showed no detectable activity for this reaction,[16b] prompting an alternative exploratory approach based on combinatorial chemistry to identify favorable sequences.

Library Design, Synthesis, and Screening. A 65 536-member combinatorial library of third-generation peptide dendrimers was prepared following our combinatorial approach to peptide dendrimers.[23] Variable amino acids at the core positions X^{1-4} included nucleophilic (His, Cys) and cationic (Arg) residues for binding and catalysis (Figure 2). Aromatic residues (Tyr, Phe, Trp) were placed in the outer positions X^{5-8} to assist substrate binding. Small and polar, negatively charged, and hydrophobic residues were distributed evenly. The library was prepared on a 400 mg batch of tentagel resin and capped by acetylation after removal of the last Fmoc protecting group. The quality of the library was checked by submitting randomly picked beads to amino acid analysis, which gave the expected average distribution of amino acids at variable positions.

The peptide dendrimer library was first screened with the fluorogenic butyrate ester **1b** by soaking the beads with an aqueous buffered solution of the substrate and plating out on a silica gel plate. Strongly green fluorescent beads appeared after ~30 min incubation on the plates and were picked for sequencing. Sequence assignment from amino acid analysis was successful in approximately 80% of the analyzed beads (Table 1). The sequences displayed at least one histidine or arginine residue at position X^2 and X^4, combined with predominantly aromatic residues at the outer positions X^6−X^8. Dendrimer sequences with one or two arginines but lacking the critical catalytic histidine residue probably showed positive in the assay due to product binding. On the other hand, sequences with at least one histidine residue presumably indicated catalytically active peptide dendrimers. The library was also screened against the undecanoyl ester **1d** to probe the possibility of lipase-like activity in the dendrimers. In this case, sequencing of fluorescent beads in the assay gave a consensus for dendrimers bearing three histidine residues at positions X^1 and X^3, combined with

Table 4. Kinetic Parameters for Ester Hydrolysis[a]

	$100 \times k_{cat}$ (min^{-1})				k_{cat}/k_{uncat}				K_M (μM)				k_{cat}/K_M (M^{-1} min^{-1})			
	citrate 5.5		Bis-Tris 6.9		citrate 5.5		Bis-Tris 6.9		citrate 5.5		Bis-Tris 6.9		citrate 5.5		Bis-Tris 6.9	
compd	**1a**	**1b**	**1a**	**1b**	**1a**	**1b**	**1a**	**1b**	**1a**	**1b**	**1a**	**1b**	**1a**	**1b**	**1a**	**1b**
R-G0	1.1	0.8	0.84	–	440	600	26	–	580	720	2200	–	18	12	3.8	1.2
R-G1	5.8	4.6	6.7	–	2400	3300	210	–	410	560	220	–	140	81	310	210
R-G2	1.2	0.79	2.1	1.9	510	570	66	150	83	110	60	110	150	70	350	70
R-G3	0.47	0.20	4.2	1.5	190	150	130	120	100	74	60	32	46	27	700	470
RM-G0	1.3	0.76	2.4	2.1	550	550	75	160	1250	910	290	390	11	8.3	82	53
RM-G1	1.1	0.69	1.9	1.8	460	500	60	140	300	250	86	120	37	28	220	150
RM-G2	0.83	0.60	2.0	2.7	340	430	63	210	69	96	61	104	120	62	330	260
RM-G3	0.29	0.08	1.7	2.3	120	60	54	180	130	25	77	27	22	34	220	860
H-G0	1.6	1.4	–	0.5	660	970	130	39	450	600	–	1200	35	22	4.5	4.3
H-G0	1.3	1.0	–	0.036	540	720	60	2.7	530	620	–	140	25	16	2.6	2.5
H-G1	1.7	1.3	3.8	3.2	680	960	120	250	550	660	790	1200	30	20	48	28
H-G1	8.1	6.4	8.6	22	3300	4600	270	1700	405	440	490	1300	200	150	170	170
H-G2	3.0	1.3	2.6	4.7	1200	960	81	360	160	82	150	470	180	160	180	99
H-G3	1.6	1.3	2.5	3.2	670	930	77	240	240	210	300	330	66	63	82	98
HM-G1	2.0	1.5	2.7	4.1	840	1100	83	310	300	300	380	750	69	50	71	54
HM-G2	1.3	1.0	2.5	6.0	540	700	77	460	59	50	150	760	220	200	170	79
HM-G3	1.6	1.3	2.9	3.3	650	910	90	250	180	190	390	320	85	68	74	100
A1[b]		3.1		1.5		2200		120		450		360		69		42
A3[b]		24		26		17000		2000		63		63		3800		4100

[a] Conditions: 3.3, 5.0 or 10 μM catalyst, 30−1000 μM substrate **1a** or **1b**, 10 mM aq Bis-Tris buffer pH 6.9, or 5 mM citrate buffer pH 5.5, 34 °C. The formation of **2** was followed by fluorescence at $\lambda_{ex} = 450$ nm, $\lambda_{em} = 530$ nm. Under these conditions, the background rate is k_{uncat} (**1a**, pH 5.5) $= 2.4 \times 10^{-5}$ min^{-1}, k_{uncat} (**1a**, pH 6.9) $= 3.2 \times 10^{-4}$ min^{-1}, and k_{uncat} (**1b**, pH 5.5) $= 1.4 \times 10^{-5}$ min^{-1}; k_{uncat} (**1b**, pH 6.9) $= 1.3 \times 10^{-4}$ min^{-1}. [b] Data for **A1** and **A3** from ref 16. Dendrimer **A1**: $(AcHisSer)_2(DapHisSerNH_2)$, Dendrimer **A3**: $(AcHisSer)_8(DapHisSer)_4(DapHisSer)_2DapHisSerNH_2$. The parameters are derived from Lineweaver−Burk plots with eight data points with $r^2 > 0.95$. The corresponding plots are given in the SI. The error on k_{cat}/K_M is approximately ±10−20% based on triplicate measurements.

Table 5. Compaction Factors *C* of Proteins and Denatured Peptides and Peptide Dendrimers As Determined by Diffusion NMR

peptide	no. of residues	radius (nm)	C
R-G3	37	1.44	0.76
RM-G3	39	1.52	0.65
H-G3	37	1.56	0.45
HM-G3	39	1.62	0.40
bovine pancreatic trypsin inhibitor[b]	58	1.58	0.95
hen lysozyme[b]	129	2.05	0.93
horse cytochrome c (NaCl-induced molten globule)[b]	104	2.01	0.86
sperm whale apomyoglobin pH 4 (molten globule)[b]	153	2.53	0.74
residues 2-38 from D3 of fibronectin binding protein[b,c]	32	1.55	0.15
hen lysozyme[b,c]	129	3.46	0.04

[a] The compaction factors were calculated from the hydrodynamic radii as described in ref 31. All data are for ca.1 mM aqueous solution (D_2O). [b] Data from ref 31. [c] Determined under strong denaturing conditions.

predominantly hydrophobic residues at positions X^6-X^8 and a threonine residue at position X^5. All sequences of active beads displayed at least one histidine residue, as expected from the requirement for esterolytic activity with the substrates.

Synthesis and Characterization of Library Hits. Dendrimers $(AcTyrThr)_8(DapTrpGly)_4$ $(DapArgSer)_2DapHisSer$ (**RG3**) with a single histidine at X^2 and two arginines at X^4, and $(AcIlePro)_8(DapIleThr)_4(DapHisAla)_2DapHisLeu$ (**HG3**) with three histidines at X^2-X^4, were resynthesized as representative members of the screening results with substrates **1b** and **1d**, respectively. The syntheses were carried out on Rink-amide resin. The dendrimers were deprotected, cleaved from the resin, purified by preparative HPLC, and investigated as soluble dendrimers in aqueous buffer. The dendrimers catalyzed the hydrolysis of substrates **1a**−**d**; however, the activity was very low with the long chain ester substrates **1c** and **1d**. The low activity of dendrimer **HG3** with **1d** contrasts with the activity observed during screening and might be caused by the much lower dendrimer concentration in this assay compared to the situation on the beads. The dendrimers were therefore further studied using the more reactive substrates **1a** and **1b**.

Both dendrimers catalyzed the hydrolysis of **1a**/**b** with saturation kinetics and multiple turnover. The pH−rate profile of **RG3** in the accessible range pH 5.5−7.5 showed a pH-independent K_M and a pH-dependent increase in k_{cat} (Figure 3). This pH-dependence is consistent with a guanidinium−sulfonate salt bridge[25] for substrate binding and the histidine side-chain as a free base triggering catalysis. Similar arginine−sulfonate interactions have been proposed in the binding of coenzyme M to hydrogenases[26] and the binding of the hapten naphthalene-1,5-disulfonate to an antibody.[27] In the case of **HG3**, the pH−rate profile showed that both K_M and k_{cat} increased with pH. This suggests that the three histidines control both binding and catalysis in this dendrimer.

For both dendrimers the mechanism of esterolysis probably involves binding of the sulfonate groups of the substrate to the pair of arginine or protonated histidine residues at position X^4, positioning the reacting acyl group in the substrate close to a histidine side chain at position X^2 which catalyzes hydrolysis

(25) Schug, K. A.; Lindner, W. *Chem. Rev.* **2005**, *105*, 67−113.
(26) Clark, D. D.; Boyd, J. M.; Ensign, S. A. *Biochemistry* **2004**, *43*, 6763−6771.
(27) Hotta, K.; Wilson, I. A.; Hilvert, D. *Biochemistry* **2002**, *41*, 772−779.

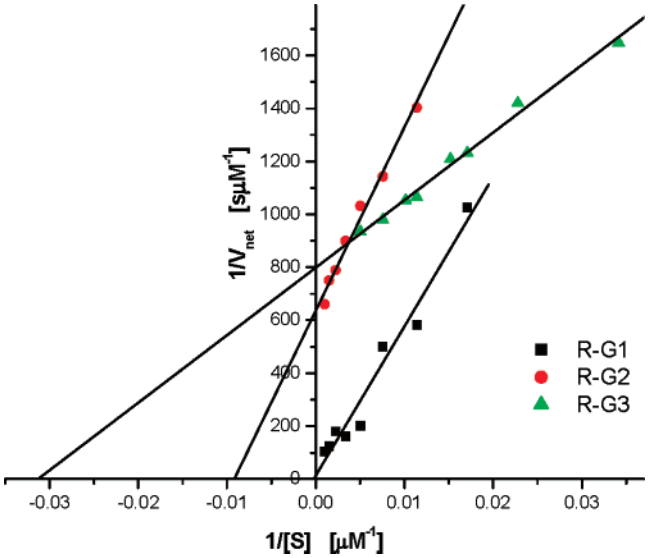

Figure 6. Michaelis−Menten plot for dendrimers **RG1**, **RG2**, **RG3** at pH 6.9 with substrate **1b**. Conditions as in Table 4.

of the acyl group as a nucleophile or general base (Figure 1). Molecular dynamics simulations using GROMACS[28] for dendrimer **RG3** and its analogue **RMG3** (see below) suggest that although the dendrimers adopt multiple conformations in aqueous solution, the pair of arginine residues and the catalytic histidine should be found mostly at the dendrimer surface in a relative orientation compatible with recognition and esterolysis of the pyrene trisulfonate substrates according to the proposed mechanism (Figure 4).

Synthesis of Dendrimer Analogues. The role of the dendritic structure on catalysis by **RG3** and **HG3** was investigated by gradual stripping of the outer branches to form the second-generation dendrimers **RG2** and **HG2,** the dendritic catalytic core **RG1**, **HG1**, and **HG1′** (an analogue of **HG1** with an His→Ala exchange at position X^2), and finally the linear core peptides **RG0**, **HG0**, and **HG0′** (an analogue of **HG0** with deletion of Leu at position X^1) (Figure 5). The spacing between the core histidine residue at position X^2, presumably responsible for nucleophilic catalysis, and the pair of arginine or histidine residues at position X^4 that probably participate in substrate binding to the sulfonate groups, might also be expected to influence catalysis. To investigate this point, we prepared two related series **RMG0→RMG3** and **HMG0→HMG3** with an additional glycine residue after the first branching. All dendrimers and peptides were prepared by solid-phase peptide synthesis and obtained in satisfactory purity after preparative HPLC purification (Table 3).

Positive Dendritic Effect in Catalysis by the R-Series Core Active Site Dendrimers. Michaelis−Menten parameters were determined for all dendrimers and lower generation analogues for substrates **1a** and **1b** in aqueous buffers at pH 5.5 and pH 6.9 (Table 4, Figure 6 and 7). The catalytic effects observed in terms of rate acceleration k_{cat}/k_{uncat} and catalytic proficiency k_{cat}/K_M were generally higher at the higher pH value, in agreement with the pH−rate profile analysis. The strongest catalytic effects were observed with the third-generation dendrimer **RG3** and its analogue **RMG3** at pH 6.9. Under these conditions the single catalytic histidine at the core is mostly present as free base while the pair of arginine residues are positively charged and probably assist in substrate binding. The catalytic proficiency however decreased in the lower generation dendrimers **RG2/RG1** and **RMG2/RMG1** which also contain these three residues in the same relative arrangement and was even lower in the linear core analogues **RG0** and **RMG0**. The positive effect of the outer dendritic layers on catalytic proficiency k_{cat}/K_M was particularly strong with the butyrate substrate **1b** in the series **RG0→RG3**, in which the third-generation dendrimer **RG3** was 390-fold more active than its linear core analogue **RG0**. In both series the outer dendritic layers enhanced catalysis by an increase in substrate binding (lower K_M) at approximately constant k_{cat}.

The positive effect of the outer dendritic layers on catalysis in the **R**-series dendrimers at pH 6.9 was not observed at pH 5.5, under which conditions the best catalysis was observed at the level of the first-generation dendrimers **RG1** and **RMG1**. Although addition of the outer denritic layers caused an increase in substrate binding comparable to that observed at pH 6.9, the catalytic rate constant k_{cat} decreased strongly, in particular upon addition of the third layer to form **RG3** and **RMG3**. The outer dendritic layers in the **R**-series dendrimers consist of a 4-fold tryptophan-glycine dyad at **G2** and an 8-fold tyrosine-threonine dyad at **G3**. The increase in substrate binding observed upon addition of these layers might be triggered by enhanced hydrophobic substrate−dendrimer interactions. The hydrophobic nature of the amino acids in **G2** and **G3** might also explain the low k_{cat} values observed at pH 5.5, considering that the ester hydrolysis reaction is favored in a highly polar medium. Indeed several previous attempts to combine aromatic residues with histidines in multivalent peptide dendrimer esterases did not produce active catalysts.[15b] The positive effect of the aromatic layers **G2** and **G3** on catalytic proficiency at pH 6.9 is therefore particularly remarkable and might reflect the onset of a catalytically favorable conformation upon neutralization of the histidine side-chain at the higher pH value.

Effects of the Dendritic Layers in the H-Series Dendrimers. The exceptional nature of the positive dendritic effect observed by addition of the noncatalytic outer layers on the catalytic core in the **R**-series was further highlighted by the catalytic behavior of the **H**-series dendrimers featuring a three-histidine catalytic core surrounded by outer layers of hydrophobic amino acids and proline (**G2** = 4 × Ile-Thr, **G3** = 8 × Ile-Pro). In this series the best catalysts were the first-generation dendrimers **HG1/HMG1** at pH 5.5 and the second-generation dendrimers **HG2/HMG2** at pH 6.9. Addition of the third dendritic layer either had a negligible effect (substrate **1b** at pH 6.9) or reduced catalytic proficiency (**1a** at pH 6.9 and **1a/b** at pH 5.5) by influencing both the catalytic rate constant (lower k_{cat}) and substrate binding (higher K_M).

Single-Site versus Multivalent Esterase Dendrimers. The most active core active site dendrimer catalysts as measured by the catalytic proficiency k_{cat}/K_M were the third-generation dendrimers **RG3** with substrate **1a** and **RMG3** with substrate **1b**. The catalytic proficiency **RMG3** at pH 6.9 (k_{cat}/K_M = 820 M^{-1} min^{-1}, Table 4) is 5-fold lower than our previously reported multivalent esterase dendrimer **A3** ($(AcHisSer)_8(DapHisSer)_4$-$(DapHisSer)_2DapHisSerNH_2$), which displayed 15 catalytic

(28) (a) Berendsen, H. J. C.; van der Spoel, D.; van Drunen, R. *Comput. Phys. Commun.* **1995**, *91*, 43−56. (b) Lindahl, E.; Hess, B.; van der Spoel, D. *J. Mol. Model.* **2001**, *7*, 306−317.
(29) DeLano, W. L. The PyMOL Molecular Graphics System (2002) DeLano Scientific, San Carlos, CA. http://www.pymol.org.

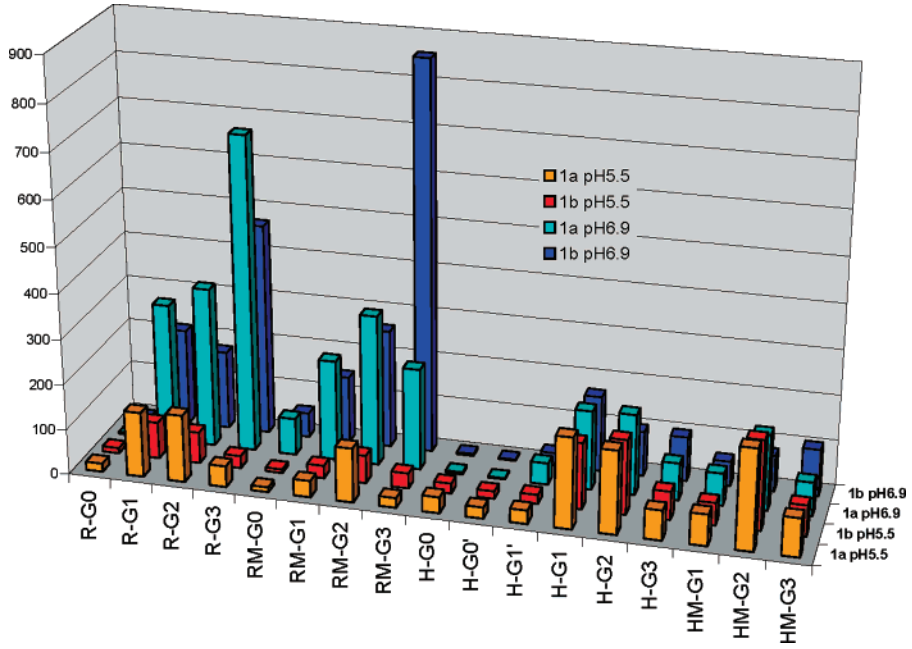

Figure 7. Catalytic proficiency k_{cat}/K_M of peptide dendrimers with acetate ester substrate **1a** and butyrate ester substrate **1b** at pH 5.5 and pH 6.9. Data from Table 4. The second-order rate constant for catalysis by 4-methylimidazole is k_2 (**1a**) = 11 M^{-1} min^{-1} and k_2 (**1b**) = 8.6 M^{-1} min^{-1} (pH 6.9).

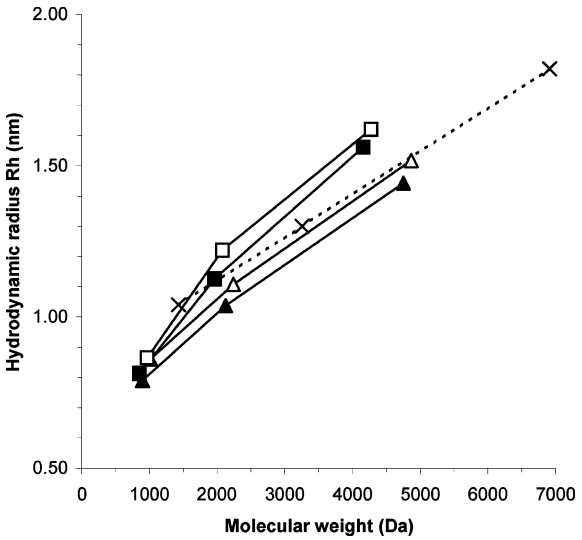

Figure 8. Hydrodynamic radii (Rh) measured by diffusion NMR spectroscopy as a function of dendrimer molecular weight. (▲) **RG1**−**3**; (△) **RMG1**−**3**; (■) **HG1**−**3**; (□) **HMG1**−**3**. The Rh were determined from the diffusion coefficients D at 5 mg mL^{-1} peptide dendrimer in D_2O at 300 K. The estimated error on Rh is ±2.6%; see Experimental Section and SI for details. (×) PAMAM dendrimers measured in MeOH (data from ref 32a).

histidines and acquired a high catalytic efficiency by cooperativity effects between these residues forming five active sites.[16] Considering that the single site dendrimer **RMG3** features only a single histidine residue, its catalytic activity is thus comparable to that of dendrimer **A3** when counted per catalytic site. On the other hand, lowering of the pH from 6.9 to 5.5 reduced the catalytic proficiency of **RMG3** by protonation of the catalytic histidine, which lowers k_{cat} at constant K_M but had almost no influence on the catalytic proficiency of the multivalent histidine dendrimer **A3**, its core analogue **A1**, or dendrimers in the **H**-series, which all feature three histidine residues in a similar relative arrangement. As a consequence, these polyhistidine dendrimers show higher rate acceleration over background at this lower pH value.

Diffusion-NMR. The very different behavior of the **R**- and **RM**-series versus the **H**- and **HM**-series dendrimers is in part due to the difference between their catalytic cores. On the other hand, the very different nature of their outer layers reflecting different selections during the combinatorial experiment might also cause a different structural behavior. To test this hypothesis, the dendrimers were investigated by diffusion NMR spectroscopy.[30] This analysis allows one to determine the average hydrodynamic radius of macromolecules in solution and has been used to characterize native and denatured proteins[31] as well as various dendrimers.[32] The dendrimers were investigated as 5 mg mL^{-1} solutions in D_2O (>1 mM). All dendrimers were fully soluble under these conditions, and the diffusion NMR data showed that all species were monomeric in solution.[33] The increase in hydrodynamic radius as a function of molecular weight for the series **RG1**→**RG3** and **RMG1**→**RMG3** was comparable to that reported for PAMAM dendrimers. By contrast, the hydrodynamic radius increased much faster with MW in the series **HG1**→**HG3** and **HMG1**→**HMG3** (Figure 8). With 37−39 residues, the third-generation dendrimers can also be compared to proteins, whose hydrodynamic radius as

(30) Cohen, Y.; Avram, L.; Frish, L. *Angew. Chem., Int. Ed.* **2005**, *44*, 520−554.
(31) Wilkins, D. K.; Grimshaw, S. B.; Receveur, V.; Dobson, C. M.; Jones, J. A.; Smith, L. J. *Biochemistry* **1999**, *38*, 16424−16431.
(32) (a) Newkome, G. R.; Young, J. K.; Baker, G. R.; Potter, R. L.; Audoly, L.; Cooper, D.; Weis, C. D.; Morris, K.; Johnson, C. S., Jr., *Macromolecules* **1993**, *26*, 2394−2396. (b) Young, J. K.; Baker, G. R.; Newkome, G. R.; Morris, K. F.; Johnson, C. S., Jr. *Macromolecules* **1994**, *27*, 3464−3471. (c) Ihre, H.; Hult, A.; Söderlind, E. *J. Am. Chem. Soc.* **1996**, *118*, 6388−6395. (d) Hecht, S.; Vladimirov, N.; Fréchet, J. M. J. *J. Am. Chem. Soc.* **2001**, *123*, 18−25. (e) Jeong, S. W.; O'Brien, D. F.; Orädd, G.; Lindblom, G. *Langmuir* **2002**, *18*, 1073−1076. (f) Fritzinger, B.; Scheler, U. *Macromol. Chem. Phys.* **2005**, *206*, 1288−1291. (g) Wong, S.; Appelhans, D.; Voit, B.; Scheler, U. *Macromolecules* **2001**, *34*, 678−680. (h) Ong, W.; Grindstaff, J.; Sobransingh, D.; Toba, R.; Quintela, J. M.; Peinador, C.; Kaifer, A. E. *J. Am. Chem. Soc.* **2005**, *127*, 3353−3361.
(33) Addition of hydroxypyrene-trisulfonates to solutions of **RG3** and **RMG3** lead to precipitation precluding the determination of hydrodynamic radii for the dendrimer−substrate complexes. Precipitation was also observed upon attempted microcalorimetric measurements with these dendrimers.

determined by NMR is larger in the denatured state than in the native state. Analysis in terms of the compaction factor *C*, as defined by Wilkins et al.,[31] shows that **RG3** and **RMG3** have a compaction factor typical for a molten globule state of proteins, while **HG3** and **HMG3** have a lower compaction factor suggesting a more disordered conformation (Table 5). The relatively tight packing of the **RG3/RMG3** dendrimers might be related to the catalytically productive effects of the outer dendritic layers on catalysis observed at neutral pH.

Conclusion

In summary, the first core active site esterase peptide dendrimers were discovered by activity screening of a combinatorial library of dendrimers designed to present catalytic residues at the core combined with hydrophobic and aromatic residues in the outer layers, thus overcoming difficulties encountered previously in our attempts to combine histidine residues with hydrophobic and/or aromatic residues to obtain dendritic esterase models.[15b−c] Catalytically productive interactions between the catalytic core and the outer dendritic layers containing aromatic amino acids occur in dendrimers **RG3** and **RMG3**, such that these third-generation dendrimers are more active than the corresponding catalytic cores **RG1/RMG1** and the second-generation dendrimers **RG2/RMG2**. By contrast, no such productive interactions occur in dendrimers **HG3** and **HMG3** where the outer dendritic layers feature hydrophobic amino acids and proline, such that their catalytic activity is already fully present in the first-generation core dendrimers **HG1/HMG1**. The different influence of the outer dendritic layers in **R**- versus **H**-series dendrimers might be related to the different degree of compaction of the dendrimers in the two series as suggested by the hydrodynamic radii determined by diffusion NMR. The possible relationship between packing and function in peptide dendrimers provides an attractive hypothesis for further investigations of dendrimers as models for proteins.

Experimental Section

Dendrimer Synthesis. Peptide dendrimers were synthesized by the Fmoc strategy according to standard solid-phase procedure and purified by preparative reverse-phase HPLC. Details of the synthetic procedure for library and single dendrimers and all characterizations are described in Supporting Information.

Assays and Kinetic Measurements. Kinetic measurements were carried out using a CytoFluor Series 4000 multiwell plate reader from PerSeptive Biosystems. Dendrimers were used as 10 μM, 15 μM, or 30 μM freshly prepared solutions in milliQ water. Solutions were prepared by dissolving the dry TFA salts of dendrimers. Substrate solutions for the Michaelis−Menten kinetics were prepared by serial dilution by a factor 2/3 (7×) of a freshly prepared 3.0 mM solution of substrate in milliQ water (final concentration on the plate 60−1000 μM). Low K_M determinations were carried using 30−200 μM final substrate concentrations, prepared by serial dilution by factors 2/3 and 1/2. Eight solutions of 8-hydroxypyrene-1,3,6-trisulfonic acid sodium salt **2** ranging from 0 μM to 100 μM in buffer were used for the calibration curve. Bis-Tris 30 mM or citrate 15 mM was used as buffer, and the pH was adjusted to the desired value with HCl 1.0 M and NaOH 1.0 M using a Metrohm 692 pH/ion meter. In a typical experiment, using a multichannel pipet, 40 μL of dendrimer was mixed with 40 μL of buffer and 40 μL of substrate in a Costar flat-bottom polystyrene 96-well-plate (150 μL). The formation of **2** was followed by fluorescence emission using absorbance filter 450/50 and emission filter 530/25. The gain was adjusted using the signal of the calibration curve prior to every experiment (typically a signal 45 000−55 000 for the 100 μM **2** well). The calibration curve (40 μL of **2**, 40 μL of buffer, and 40 μL of H_2O) and the blank (40 μL of substrate, 40 μL of buffer, and 40 μL of H_2O) were recorded for every experiment in the same time. The temperature inside the instrument was adjusted to 34.0 °C. Kinetic experiments were followed for typically 180 min. The data points were measured every 90 s. Fluorescence data were converted to product concentration by means of the calibration curve. Initial reaction rates were calculated from the steepest linear part observed in the curve that gives fluorescence *versus* time, typically between 500 and 2000 s, corresponding to less than 10% conversion.

Measurement of Apparent Rate Enhancements and Kinetic Parameters k_{cat} and K_M. V_{cat} is the apparent rate in the presence dendrimer catalyst; V_{un} is the rate in buffer alone. The observed rate enhancement is defined as V_{net}/V_{un} with $V_{net} = V_{cat} - V_{un.}$ Michaelis−Menten parameters k_{cat} (rate constant) and K_M (Michaelis constant) were determined from the linear double reciprocal plot $1/V_{net}$ versus 1/[S] (where [S] is the substrate concentration). The rate constant k_{uncat} without catalyst was calculated from the slope of the linear curve that gives V_{un} (as product concentration per time) *versus* substrate concentration [S].

***k*$_2$ (4-Methylimidazole).** The solutions of 4-methylimidazole were prepared by serial dilution from a stock solution (3.0 mM) adjusted to the desired pH value using HCl 1 M. The reaction rate with 4-methylimidazole (4-MeIm) was obtained under the same conditions as described above. The final concentrations in the plate were 0, 87.9, 132, 198, 296, 444, and 667 μM 4-MeIm, 200 μM of substrate, and 10 mM of buffer. The second-order rate constants k_2 were calculated from linear regression of the experimentally measured pseudo first-order rate constants k' as a function of 4-MeIm concentrations. The second-order rate constants k_2 is given by $k_2 = k'/[S]$, where [S] indicates the concentration of substrate.

Diffusion NMR Measurements. The standard PGSE diffusion NMR experiments were performed by the NMR service of the Department of Chemistry and Biochemistry of the University of Bern. The measurements were carried using a Bruker DRX400 or DRX500 with dilute solutions (typically 5 mg/mL) in D_2O at 300 K. The gradient with a maximum strength of 50×10^{-4} T cm^{-1} was calibrated using the HOD proton signal in 99.997% D_2O. The diffusion time Δ was 50 ms and the gradient duration δ was 7 ms. The diffusion coefficient *D* was derived from peak integrals or intensities using the Simfit software from Bruker. The hydrodynamic radii were calculated from the diffusion coefficient *D* using the Stokes−Einstein equation[30] with $\eta = 1.089$ mPa for D_2O at 300 K. The compaction factor was calculated as originally proposed.[31] See the Supporting Information table for values and errors.

Acknowledgment. This work was financially supported by the University of Berne, the Swiss National Science Foundation, and the European Marie-Curie Training Network IBAAC.

Supporting Information Available: Synthetic procedures and HPLC, MS (ES+), and ^{1}H NMR analysis of all dendrimers and peptides synthesized, Michaelis−Menten plots for each data point, and diffusion coefficients for the dendrimers. This material is available free of charge via the Internet at http://pubs.acs.org.

JA074115F